Aalborg Universitet

AALBORG UNIVERSITY

Shadow Fading Spatial Correlation Analysis for Aerial Vehicles

Ray Tracing vs. Measurements

Lechuga, Melisa Maria Lopez; Sørensen, Troels Bundgaard; E. Mogensen, Preben; Wigard, Jeroen; Kovács, István Z.

Link to publication from Aalborg University

Shadow Fading Spatial Correlation Analysis for Aerial Vehicles: Ray Tracing vs. Measurements

Melisa López*, Troels B. Sørensen*, Preben Mogensen*†, Jeroen Wigard†, István Z. Kovács†

*Aalborg University

{mll, tbs, pm}@es.aau.dk

†Nokia Bell Labs

{istvan.kovacs, jeroen.wigard}@nokia-bell-labs.com

Abstract—Although the use of cellular networks to serve drones has been investigated in several recent works, the path loss or shadowing variation is still relatively unexplored. The variation and its dynamic behaviour is of importance in characterizing the reliability of the drone communication link, but difficult to assess by experimental means on a large scale. The main goal of this paper is to study the feasibility of ray tracing models to accurately predict shadow fading variations at different heights, so that the shadow fading correlation distances for the UAV channel can be found in both vertical and horizontal directions, without the need of performing extensive field measurement campaigns. For that, predictions obtained through a ray tracing tool are compared to field measurements in an urban scenario. Our results show that with accurate 3D maps, the tool is useful for predicting the dynamics of the UAV propagation channel, and therefore can be used partly as a substitute for field measurements.

Index Terms—Ray tracing, UAVs, drone, aerial vehicles, shadow fading, urban measurements, propagation prediction, field measurement, drone communication.

I. Introduction

The 5th Generation (5G) New Radio (NR) cellular system is expected to serve a wide range of services. Mission-critical communications, where reliability and a short-time response of the system is needed typically for safety reasons [1], is expected to be one of those services. Some examples would include vehicle-to-everything (V2X) communications, railway communications or the Command and Control (C2) link for unmanned aerial vehicles (UAVs). All the three examples are characterized by high mobility. Long-Term Evolution (LTE) and 5G networks investigations for meeting the requirements of such type of communication [2]-[4] have been carried out.

The application of interest in this paper is the use of LTE/5G for serving the control link of UAVs. There are multiple UAV uses such as transport of medical goods, rescue services, inspection of telecommunications infrastructure, to name a few [5]. All the mentioned use cases are more attractive if a UAV can fly Beyond Visual Line-Of-Sight (BVLOS) of the controller, i.e., allowing the UAV to be controlled from a remote pilot location. For public safety reasons, it is expected that reliability will be a major requirement for BVLOS operation. One of the consequences of this requirement is that the drones, as they are also commonly known, need to be connected to a flight control unit, through the C2 link, which carries mainly flight-related information. The existing cellular networks are a

potential option to provide such communication, since their coverage is ubiquitous, and they are already serving many cellular network users, and therefore provide a cost-efficient option. Connection reliability in cellular networks is impacted not only by the coverage provided, but also by the dynamic behaviour of the coverage, for what concerns both desired and interfering signals. The dynamics impact for example the radio mobility which determines cell selection, reporting and handovers.

There are already several publications such as [6]-[8] where the radio performance of drones when using cellular networks for the C2 link and some potential interference mitigation schemes are studied. A path loss model for the radio channel between the UAV and cellular networks is proposed in [6],[8],[14]. This height dependent model, based on measurements, suggests a path loss exponent and shadowing which decrease as the UAV height increases. Whereas path loss characterises the (static) large-scale effect, it is also important to consider and model the temporal and/or spatial dynamic effects in propagation, to realistically evaluate connection reliability when the drone moves through airspace. These dynamic effects are typically characterised by the standard deviation, and the correlation properties of shadow fading. There is a need to have more empirical evidence for the study of correlation properties of the radio channel in aerial scenarios. However, achieving this purely by experimental procedure is difficult, given the practicalities in conducting drone flights, particularly in urban environments.

In this paper, we present a large-scale study at different heights, with a multiple transmitters scenario, on the accuracy of the ray tracing tool when predicting shadowing variations by comparing it to field measurements.

The paper is organized as follows: Section II introduces the ray tracing models analysed in this study, the measurement setup and the scenario. Results, discussion and conclusions are followed, respectively, in Sections III, IV and V.

II. Methodology

A. Field Measurements

To be able to compare ray-tracing predictions with real channel measurement samples, field measurements were required. Two measurement campaigns were performed in a live LTE network in the 1800 MHz frequency band: a drive test
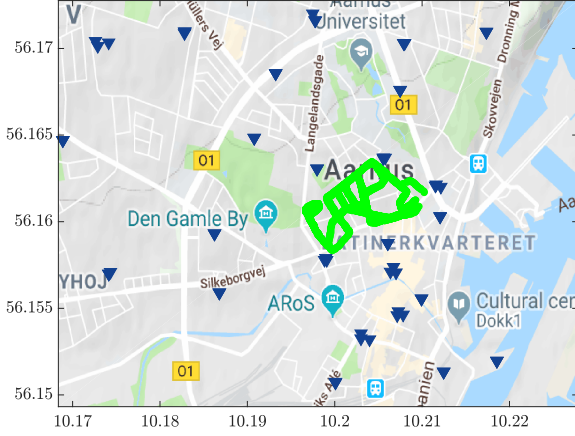
Fig. 1. Measurement route (in green) in Aarhus (Denmark), including LTE network sites location provided by a local operator.

Fig. 2. Measurement set up for the drone campaign.

campaign at ground level and an airborne campaign with a drone at different heights. Both campaigns were performed in a small area of approximately 0.25 km^2 in the city center of Aarhus, in Denmark, where 17 different locations where measured. The studied area is hilly, and the terrain elevation in the topographic maps varies between 0 m and 27 m. As it is show in Fig. 1, the network in this area consists of 23 tri-sectorial sites with heights between 15 m and 60 m and average Inter-Site Distance (ISD) of 470 m. Full information of the cells including antenna tilt, orientation, etc., provided by the network operator was used for the study.

In both measurement campaigns, the car and the drone were equipped with the Rohde & Schwarz FreeRider system [12]. The scanner was equipped with an external omnidirectional antenna, mounted on the rooftop of the car, and respectively, extending about 50 cm above the drone fuselage and rotor plane, as it is shown in Fig. 2. The GPS position was logged for each measured Reference Signal Received Power (RSRP) sample.

B. Ray Tracing Model

Two different propagation models available in the AWE WinProp tool are studied: the Dominant Path Model (DPM) and the Intelligent Ray Tracing (IRT). The Authors in [10] describe the algorithm of DPM for an urban scenario, which consists of the determination of the dominant path contributing to the power reaching the receiver. They present the general performance of DPM at ground level and compare it with IRT, which considers all significant possible contributions of the different rays reaching the receiver [11]. It is a one-transmitter study, where results show that DPM considerably reduces computation time respect to IRT, and that mean value and standard deviation of the difference between measurements and predictions is not only equal but sometimes better with DPM.

For this analysis we used average signal power predictions from WinProp, which mainly depend on the propagation exponents settings: before and after breakpoint Line Of Sight (LOS) and Obstructed-LOS (OLOS). Since WinProp offers the possibility to tune these parameters by using field measurements, those obtained from the campaigns mentioned in Section II-A were used to calibrate the models. The 3D maps (including building shapes and terrain topography of the area) used in the ray tracing tool to perform this study cover an area of 8.5 km^2 with 5m resolution around the campaign area. The building database includes 10019 buildings, where the minimum height is 43 m and the maximum height is 146 m. First, calibration of the propagation exponents was performed for ground level and all the different heights, separately. Calibration in WinProp is a standard procedure and it is performed automatically [9]. It calculates the Minimum Mean Squared Error (MMSE) of the difference between measurements and predictions. The scanner samples were converted from RSRP to signal power and further averaged over 5 m, to match with the 3D maps resolution.

We show in Table I the 50%-ile value of the signal power distributions of measurements and predictions before and after calibration for the ground level case. For both cases, the models provide a better estimation of the signal power after calibration.

Calibration was performed for both DPM and IRT models, and the results for both models were analysed before and after calibration. For IRT, we first ran predictions using the default WinProp values for ground level. As the difference between calibrated DPM and default WinProp IRT propagation exponents for the ground level case was minimum, we decided to use the calibrated DPM propagation exponents to run

TABLE I
50 %-ILE OF SIGNAL POWER DISTRIBUTIONS FOR MEASUREMENTS AND PREDICTIONS - DPM AND IRT MODELS BEFORE/AFTER CALIBRATION

	Before Calibration	After Calibration
Measurements	-72.1	
DPM	-84.9	-72.1
IRT	-66.3	-72.2

| | Ground Level | | 10 m, 15 m, 30 m |
	DPM	IRT	DPM/IRT
LOS exp.	2.6	2.8	2.2
OLOS exp.	2.7	2.9	2.4
LOS exp. after breakpoint	3.5	3	3.3
OLOS exp. after breakpoint	4	3	3.3

Trasmitter ID	Mean Value [dB]	Std. Dev. [dB]
A	3.5	6.5
B	10.7	7.8
C	-0.1	5.0
D	14.5	4.7
E	-11.5	5.7
F	5.5	5.1
G	-6.1	5.0

IRT predictions at different heights. Results after calibration improved slightly only for the ground level case, whereas for the different heights the results worsened. For this reason, IRT propagation exponents shown in Table II are the calibrated values for ground level case only. For the different heights, the parameters used for IRT were the same as for DPM corresponding to the same height.

The factor for breakpoint distance determination was set to 2π as it is recommended in [9] for the urban case. The initial value for the breakpoint distance is calculated using the heights of the transmitter and receiver, and the wavelength [9]. The exponents after breakpoint distance were not determined during calibration for above ground, and therefore they were set to the default value set in the tool.

A summary of the overall standard deviation of the difference between measurements and predictions for the different heights after DPM calibration is presented in Table III. As it can be observed, the overall (including all transmitters) standard deviation of the difference between measurements and predictions is high compared to results in [10] even after calibration. To explain that, we present in Table IV a per transmitter analysis, where only some of the transmitters used for calibration of DPM at ground level are shown. The results in Table IV are obtained by subtracting, pixel by pixel, measurements to predictions for each transmitter independently. It can be noticed that, per transmitter, there is a considerable spread of the mean values, between -6.1dB to +14.5dB, which contributes to the overall high standard deviation of the difference. This will be further discussed in Section IV.

C. Shadow Fading Estimation

Once calibration was performed, we ran new predictions with the optimal propagation exponents. The results obtained from those predictions were used for the analysis presented in Section III.

Height	# of transmitters used for calibration	Std. Dev. [dB]
Ground Level	14	10.62
10	16	12.96
15	17	11.66
30	28	8.03

To analyse shadow fading, distance-dependency was removed from both measurements and predictions. The values were subsequently de-trended per transmitter prediction, so that only the variation in the local mean power level remained. Processed like this, the resulting values are therefore proportional to the shadowing in large-scale propagation.

To measure the accuracy of the predictions, we performed cross-correlation of time sequence samples between measurements and predictions. The cross-correlation coefficient, r_{y1y2}, used for this analysis is presented in Eq. (1), where c_{y1y2} represents the cross-covariance, defined in Eq. (2), of the time series $y1$ and $y2$, and $s1$ and $s2$ are the sample standard deviation of the time series $y1$ and $y2$, respectively, as it is shown in Eq. (3).

$$r_{y1y2} = \frac{c_{y1y2}(k)}{s_{y1}s_{y2}}; k = 0, \pm 1 \quad (1)$$

$$c_{y1y2}(k) = \frac{1}{T}\sum_{t=1}^{T-k}(y_{1,t} - \overline{y_1})(y_{2,t+k} - \overline{y_2}); k = 0, \pm 1 \quad (2)$$

$$s_i = \sqrt{c_{y_iy_i}(0)} = \sqrt{Var(y_i)} \quad (3)$$

The cross-correlation was performed for lags $k = 0, \pm 1$, where a lag corresponds to a pixel position (5m). This was done to take into account that measurement positioning can be off by some meters, and therefore misalign samples in the comparison. For the results, the maximum value among the cases with $k = 0, \pm 1$ was chosen.

III. RESULTS

A. Correlation Coefficients between measurements and predictions

The correlation analysis was applied per street and transmitter to get a measure for the accuracy in the prediction of the shadowing. We consider a prediction to be sufficiently accurate when the value obtained from cross-correlation in Eq. (1) is higher than 0.6. We present two examples of the measurements and predictions along a street in Figs. 3 and 4. For these cases, cross-correlation coefficients (CC) are 0.5457 and 0.8803, respectively. As it can be seen in Fig. 3, with a correlation value close to the limit we established (0.6), shadow fading is well predicted since the strongest variations
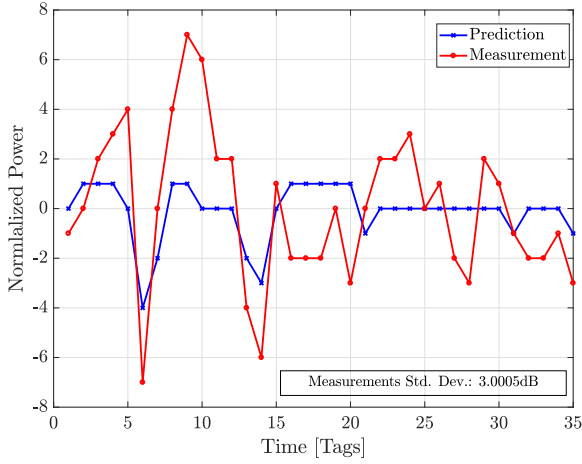
Fig. 3. Example (I) of comparison of measurement and prediction along the route. CC = 0.5457.
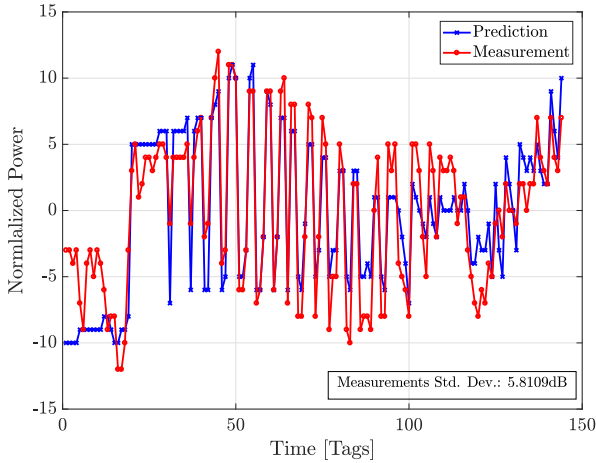

Fig. 4. Example (II) of comparison of measurement and prediction along the route. CC = 0.8803.

are seen in predictions as well as in measurements and the correlation is high in the first stretch of the street.

Figure 5 shows the CDF of the correlation coefficients of the different combinations of street-transmitter for the whole set of measurement data, for both DPM and IRT. Results are presented for four different heights: ground level (1.5m), 10m, 15m and 30m. IRT performance is better than DPM in predicting the behaviour of the measurements, as the percentile of correlation coefficients above 0.6 is higher. Prediction accuracy in terms of correlation behaviour, deteriorates with height.

B. Shadowing distribution

Figure 6 shows examples of the shadow fading (SF) distributions of both measurements and IRT predictions at ground level. They both adhere reasonably to the log-normal model with zero mean. The best-fit Gaussian is also shown for comparison. The standard deviation of the SF predictions
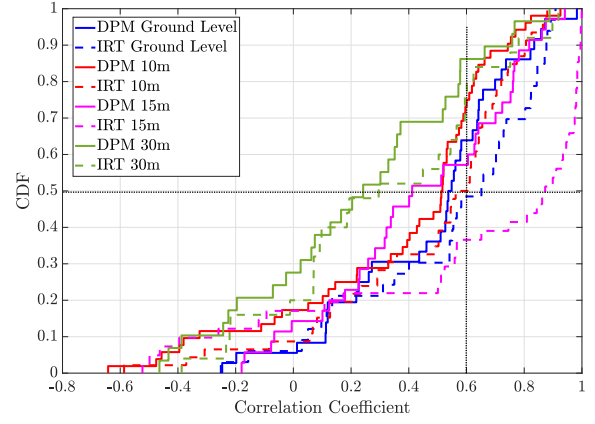

Fig. 5. CDF of cross-correlation coefficients between measurements and predictions for all measurement locations and transmitters.
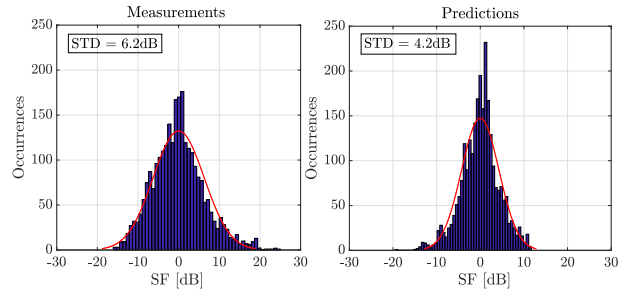

Fig. 6. SF distribution for ground level measurements and IRT predictions.

(4.2dB) is lower than for the measurements (6.2dB). This is also the observation at increased height, as shown in Fig. 7 where the mean SF standard deviation is shown versus height the different models analysed.

Fig. 7 indicates that the mean standard deviation increases up to about the rooftop level, approx. at 10m, where after it decreases due to the radio path clearance [13]. The same trend is captured by the ray tracing predictions, and therefore seems to suggest that propagation paths in the transition zone at rooftop level, are more diverse and dynamic than below and above rooftop. While at ground level, the dominant paths are mostly "street-guided", and above rooftop level they are predominantly free-space, the high standard deviation at 10 m (i.e., transition zone) suggests that there might be overlapping of "street-guided", over-rooftop and free-space contributions.

IV. DISCUSSION

Two factors impact our results. Accurate predictions naturally require maps which are representative. We found inaccuracies in our 3D maps that suggest local changes in some parts of the city in the map areas considered with respect to real layout at the time of measurements. Inaccuracies were identified in four different locations within the map, and the worst case example is shown in Fig. 8. At ground level, all the predictions with correlations lower than 0.6 have been proven to be close to areas where there are map inaccuracies.
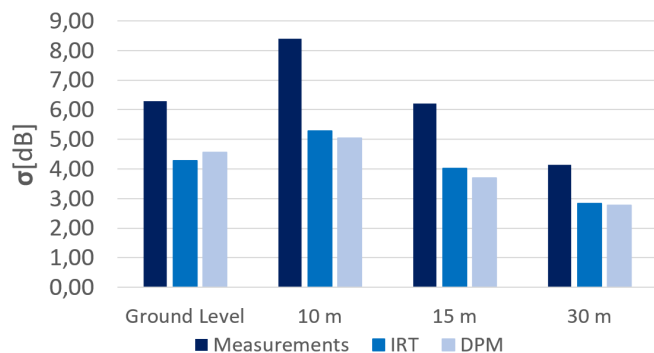
Fig. 7. Average SF standard deviation values over all transmitter-street combinations.

Fig. 8. Portion of the studied area: actual maps (top) and 3D database (bottom).

However, the same study is difficult to carry out for the different heights, as the transmitters observed by the drone are sometimes far away [6].

On the other hand, there is a limited accuracy on the building data bases [10]. The buildings are modelled as a polygonal cylinder of uniform height, where the rooftop shape is not being considered. This is surely affecting the above-rooftop predictions and explains why some of the transmitters present high mean value and standard deviation on the difference between measurements and predictions, as it is shown in Table IV. For the same reason, shadowing variation is slightly lower for the predictions than for the measurements, but it can be seen in Figs. 6 and 7 that they follow the same trend.

Despite the maps inaccuracies, results show that predictions using IRT and DPM show about the same standard deviation versus height, but IRT is better in capturing the temporal dynamics of the SF process. The cost of using the IRT model is computation time, which is considerably higher than for DPM [10].

V. CONCLUSIONS

This paper studies, by comparing with field measurements, the feasibility of ray tracing predictions and models to accurately predict shadowing variations at different heights.

From analysis and comparison of standard deviation and correlation properties, there is a good match between predictions and measurement data, the latter covering a set of different propagation conditions in an urban environment.

Overall, our study confirms that ray tracing tools can be used to obtain more empirical evidence and a better knowledge of the UAV radio channel, including shadow fading correlation properties, which play a key role in the mobility management algorithms, such as handover.

ACKNOWLEDGMENT

REFERENCES

[1] G. P. Fettweis, "The tactile internet: Applications and challenges," IEEE Vehicular Technology Magazine, vol. 9, no. 1, pp. 64-70, March 2014.

[2] T. Doumi, M. F. Dolan, S. Tatesh, A. Casati, G. Tsirtsis, K. Anchan, and D. Flore.,"LTE for public safety networks.", Communications Magazine, IEEE, 51(2):106–112, February 2013.

[3] S. Mukherjee and C. Beard, "A framework for ultra-reliable low latency mission-critical communication," 2017 Wireless Telecommunications Symposium (WTS), Chicago, IL, pp. 1-5.

[4] R. Ferrus and O. Sallent., "Extending the LTE/LTE-A business case: Mission and business-critical mobile broadband communications." Vehicular Technology Magazine, IEEE, 9(3): 47–55, Sept 2014.

[5] M. Mazur, "Clarity from above. PwC global report on the commercial applications of drone technology." [online] Available: http://www.dronepoweredsolutions.com/, May 2016.

[6] R. Amorim, H. Nguyen, P. Mogensen, I. Z. Kovacs, J. Wigard, and T. B. Sørensen, "Radio channel modeling for UAV communication over cellular networks," IEEE Wireless Communications Letters, vol. 6, no. 4, pp. 514-517, Aug 2017.

[7] I. Kovacs, R. Amorim, H. C. Nguyen, J. Wigard, and P. Mogensen, "Interference analysis for UAV connectivity over lte using aerial radio measurements," IEEE 86th Vehicular Technology Conference (VTC-Fall 2017), pp. 1-6.

[8] W. Khawaja, O. Ozdemir, and I. Guvenc, "UAV air-to-ground channel characterization for mmWave systems,"IEEE 86th Vehicular Technology Conference (VTC-Fall 2017), pp. 1-5.

[9] WinProp Manual for Version 2018.1.2 Release. Available Online: https://altairhyperworks.com/product/FEKO/WinProp-Propagation-Modeling

[10] R. Wahl, G. Wölfe, P. Wertz, P. Wildbolz, F. Landstorfer, "Dominant Path Prediction Model for Urban Scenarios,"14th IST Mobile and Wireless Communications Summit, 2005.

[11] R. Hoppe, G. Wolfle and F. M. Landstorfer, "Accelerated ray optical propagation modeling for the planning of wireless communication networks," IEEE RAWCON 99. pp. 159-162.

[12] "R&S TSME Ultracompact Drive Test Scanner", Product brochure, version 13.00 (PD 3606.7418.12), September 2017.

[13] B. V. D. Bergh, A. Chiumento, and S. Pollin, "LTE in the sky: Trading off propagation benefits with interference costs for aerial nodes," IEEE Commun. Mag., vol. 54, no. 5, pp. 44–50, May 2016.

[14] 3GPP(2018). "Study on enhanced LTE Support for Aerial Vehicles". TR36.777 v.1.1.0.